
Reprinted From

The American Society of Mechanical Engineers

PVP — Vol. 170, *Innovative Approaches to Irradiation Damage, and Fracture Analysis*

Eds.: D.L. Marriott, T.R. Mager, and W. H. Bamford

Book No. H00485 — 1989

STRUCTURAL INTEGRITY EVALUATION BASED ON AN INNOVATIVE FIELD INDENTATION MICROPROBE

F. M. Haggag, R. K. Nanstad, and D. N. Braski

Metals and Ceramics Division

Oak Ridge National Laboratory

Oak Ridge, Tennessee

ABSTRACT

A brief description is given for a field indentation microprobe (FIM) apparatus which was developed to evaluate, nondestructively in situ, the integrity of metallic structures. The FIM consists of an automated ball indentation (ABI) unit for determining the mechanical properties (yield strength, flow properties, fracture toughness, etc.) and a nondestructive evaluation (NDE) unit (consisting of ultrasonic transducers and a video camera) for determining the physical properties such as crack size, material pile-up around indentation, and residual stress presence and orientation. The laboratory version used here performs only ABI testing.

Results of the laboratory version of the FIM tests on unirradiated and irradiated A212B pressure vessel steel are discussed in this paper. Excellent agreement was obtained between yield strength and flow properties (true-stress/true-plastic-strain curve) measured by the ABI tests and those of uniaxial tensile tests.

INTRODUCTION

In order to assess the integrity of structures following accidents or severe service conditions, knowledge of the material's mechanical properties, the size and extent of induced defects, and the current thickness and residual stresses are required. This is particularly important for nuclear components such as pressure vessels and their supports because of the radiation-induced embrittlement. This was one incentive to develop a nondestructive testing apparatus such as the FIM which is described in detail in Ref. 1 and briefly presented here (together with test results on unirradiated and irradiated A212B pressure vessel steel). Other motivations are general applications, e.g., in-service examination of components such as pressure vessels and piping in nuclear and non-nuclear applications, welding characterizations, new alloy development, and when limited amounts of material are available.

The use of FIM nondestructive tests on deformed, aged, and embrittled structural components may also result in extending their useful service life based on in-situ mechanical test results rather than using simulated conditions or surveillance test data.

THE FIELD INDENTATION MICROPROBE (FIM) APPARATUS

The main components of the FIM apparatus are shown schematically in Fig. 1. The method of mounting the testing head of the FIM on the structural component is not shown since the exact mechanism will vary on a case-to-case basis depending upon the geometry and position of the particular structure. Typically a tripod mechanism having magnets or clamps can be utilized for releasable attachment to the structure. The tripod arrangement facilitates adjustment of the ball indenter to be perpendicular to the surface of the structure or test specimen. The load can be applied by hydraulic, pneumatic, mechanical, or any other means. In brief, the FIM consists of two main units: an automated ball indentation (ABI) unit for measuring the mechanical properties and a nondestructive evaluation (NDE) unit (consisting of ultrasonic transducers and a video camera) for determining the physical properties such as crack size, material pile-up around indentation, and residual stress presence and orientation. The mechanical properties measured by this innovative FIM apparatus include elastic modulus, yield strength, Lüders strain, strain-hardening exponent, ultimate strength, Brinell hardness, true-stress/true-plastic-strain curve up to 20% strain, and residual stress presence and orientation. The fracture toughness is also estimated using the ABI measured flow properties and a modified critical fracture strain model. Furthermore, the shift in the ductile-to-brittle transition temperature for steel plates and welds, e.g., due to neutron irradiation embrittlement, can be estimated from the ABI measured change in the material yield strength.

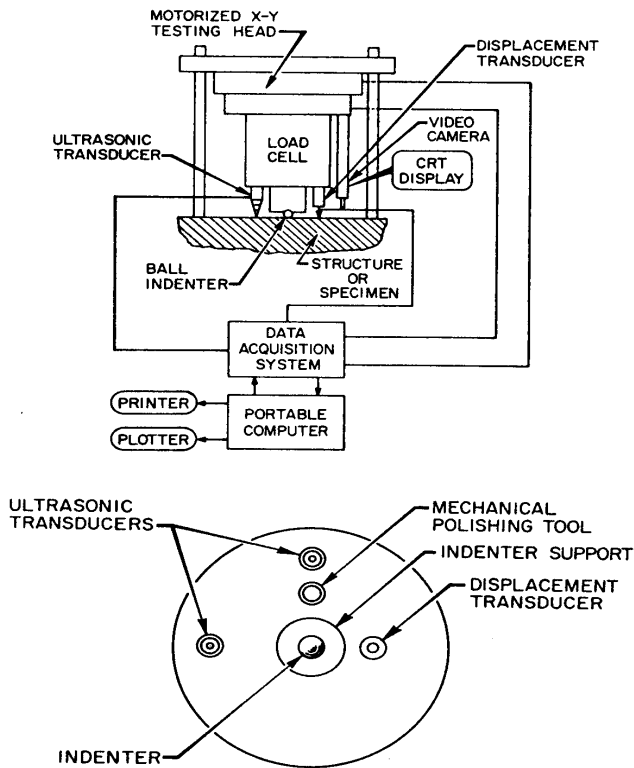


Fig. 1 Basic components of the Field Indentation Microprobe (FIM) apparatus. (a) Schematic and Block Diagram, (b) Relative positions of the testing tools mounted on the bottom of the load cell of the FIM apparatus.

THE AUTOMATED BALL INDENTATION (ABI) TEST

The ABI test is based on multiple indentations (at the same penetration location) of a polished metallic surface by a spherical indenter. This is accomplished by cyclic loading and unloading of the indenter into the test material where the load is increased in the successive loading cycles. The applied loads and associated displacements (depth of penetration of the indenter into the test specimen) are measured during both loading and unloading using a load cell and a linear variable differential transducer (LVDT). The test set-up of the current work used a 1.59-mm diameter ball indenter and a spring-loaded LVDT which were mounted to the load cell of an MTS hydraulic testing machine. Details of the ball indenter and the LVDT are shown in Fig. 2. An in-house built-in data acquisition and control system and a Hewlett-Packard computer were used for automated testing as well as acquiring and processing test data. The load-displacement data were used to determine the yield strength and produce the ABI-derived true-stress/true-plastic-strain curve. The ABI analyses are based primarily on elasticity and plasticity theories and some empirical correlations as described in Ref. 1. The primary equations used in these analyses are given in the next section. Results of ABI-derived fracture toughness estimates using the modified critical fracture strain model are presented and discussed in another paper of this symposium (Ref. 2).

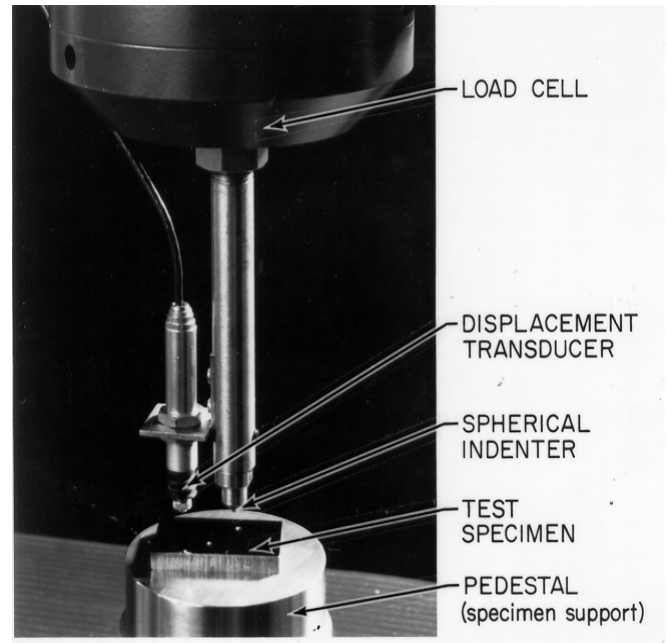


Fig. 2 Ball indenter and spring-loaded LVDT mounted to the load cell of a hydraulic testing machine (not shown in figure).

RESULTS AND DISCUSSION OF ABI TESTS

The material chosen here for conducting the ABI tests was A212B pressure vessel steel used in the fabrication of the vessel shell of the High Flux Isotope Reactor (HFIR) at the Oak Ridge National Laboratory. Details of the chemical composition and heat treatment of the unirradiated material as well as the irradiation history of the vessel and its surveillance specimens are given in Ref. 3. This material was chosen to be tested in both unirradiated and irradiated conditions for the following two reasons: (1) its apparent high embrittlement rate (as explained in Ref. 4) and (2) the applicability of its embrittlement rate effect to the evaluation of the integrity of light-water reactor pressure vessel supports as discussed in Ref. 5.

Indentation tests were conducted on specimens cut from broken halves of previously tested Charpy V-notch (CVN) specimens (see Fig. 3). The mini-tensile specimens were electric-discharge machined (EDM) from broken CVN with total length of 25.4 mm, a gage section of 7.6 mm, and a thickness of 0.76 mm (see irradiated half specimen in the horizontal glass bottle in the right corner of Fig. 3). The ABI tests conducted on the end tabs of these mini-tensile specimens using a 1.59-mm diameter ball indenter did not produce good results because of back surface effects due to their small thickness. However, remaining blocks in the form of 4.2-mm-thick mini-tensile specimens) from irradiated CVN broken halves (e.g. see block No. A96 in the vertical bottle in Fig. 3) produced good results for indentations made on their end tabs. Other specimen geometries used for bench marking ABI test results presented here and in Ref. 2 are also shown in this figure. These include a metallographic mounted specimen, a broken CVN specimen, an intact CVN specimen, and broken halves of 25.4 mm-thick and 12.7 mm-thick compact specimens. Note that the geometry of laboratory specimens for valid ABI testing must satisfy

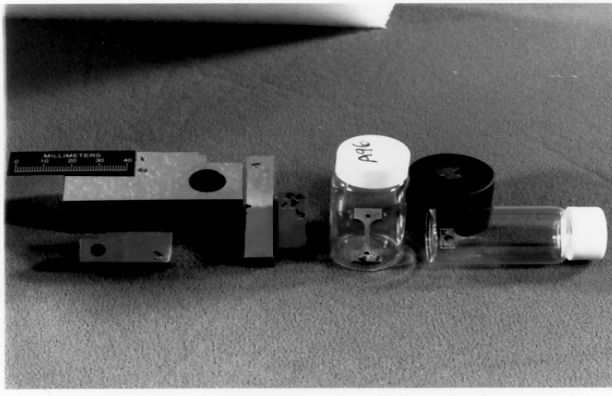


Fig. 3 Specimen geometries used in automated ball indentation (ABI) tests.

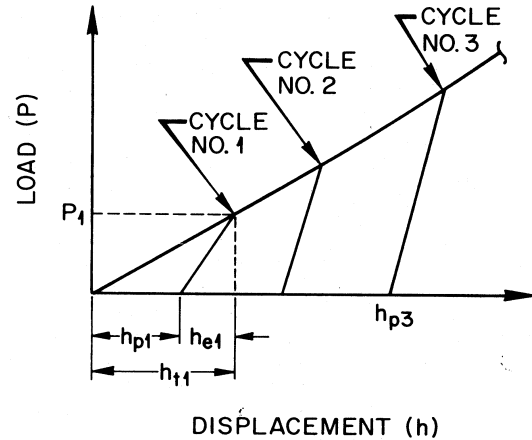


Fig. 4 Schematic representation of the relationship between load and displacement of the ball indenter of Fig. 2 as observed by increased cyclic loading.

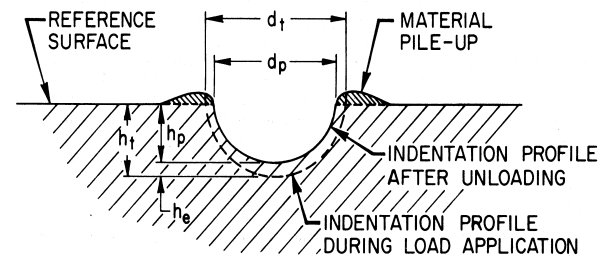


Fig. 5 Illustration of indentation geometries before and after load application (the material pile-up around the indentation is exaggerated).

thickness and area requirements around the final indentation relative to the size of the indenter. However, for actual field applications these requirements will be satisfied for most structural components. In these field cases the ABI technique offers the advantage of evaluating the mechanical properties in small localized areas such as welds and heat affected zones.

The main problem in determining yield strength from ball indentation tests is due to the Lüders strain behavior. In a uniaxial tensile test the Lüders strain is the inhomogeneous plateau (horizontal portion) of the stress-strain curve where it is confined mostly to a defined volume of the specimen gage section. Hence, the inhomogeneous (Lüders) and homogeneous (work hardening) behaviors in a tensile test are well defined and separated from each other. In contrast, in an ABI test the material has less constraint at the surface around the indentation. With increasing loads an increasing volume of material is forced to flow under multiaxial compression caused by the indenter and more material pile-up and Lüders strain occur around the indentation. Lüders strain behavior in ball indentation testing is discussed and demonstrated in Ref. 6. Thus, in an ABI test both inhomogeneous and homogeneous material behavior occur simultaneously during the entire test. Consequently, an accurate determination of yield strength should be based on the entire load-displacement curve of the ABI test as explained later. Schematics of the ABI load-displacement plot and the profile of indentation (exaggerated to show material pile-up) are shown in Figs. 4 and 5. The previous technique of Ref. 6 involved the use of a prior developed correlation (using either optical interferometry or mechanical profilometry techniques) between Lüders strain and the geometry of the lip (material pile-up) around a ball indentation in order to determine the Lüders strain and then the yield strength for a certain carbon steel material. Since such a correlation for each material does not exist and its development is expensive, the FIM does not utilize such an approach. Furthermore, the use of optical interferometry is impractical for field testing applications.

The FIM analyses use an innovative method for analyzing the load-displacement data to determine the yield strength and to produce the true-stress/true-plastic strain curve as explained below (Refs. 1, and 6, through 12).

The field indentation microprobe is utilized in the following manner. After the testing head is properly secured to the structure so that the load cell is perpendicular to the surface where testing is to be performed, this surface is prepared using the polishing tool. Thereafter, the computer causes the indenter tip to be brought into contact with the polished surface. The total and plastic indentation depths (h_{t1} and h_{p1}) and the applied indentation load (P_1) are then measured for the first cycle. Typically the load is increased for each succeeding cycle and the values of P , h_t , and h_p are measured for each cycle. Several load cycles (typically five or more) are conducted at the same indentation location for determining a full true-stress/true-plastic-strain curve at this location (data from each cycle yield a point on this curve). This cyclic loading can be continued; however, the maximum total indentation depth (h_t) should not exceed one-half of the diameter, D , of the indenter. Following the final cycle the plastic indentation diameter, d_p , can be independently measured using the video camera. If a measure of the amount of material pile-up and/or existence and orientation of residual stresses is required, thickness measurements are performed before and after indentation using the ultrasonic transducers over a traverse distance of a least one indenter diameter from each side of the indentation and in two nominally perpendicular directions. As stated above, the FIM operation is typically controlled by a program stored in the computer, and data as to the load, indentation depth, etc., measured using the data acquisition system are stored on magnetic discs in the computer for post-test processing.

The utility of the present FIM invention stems in part from its ability to derive, from depth-of-penetration and load values obtained

during cyclic and incremental loading and unloading, the essential material condition behavior. These include: true-stress/true-plastic-strain curve, strain-hardening exponent, strength coefficient, elastic (Young's) modulus, yield strength, Lüders strain, and estimates of fracture toughness.

The homogenous plastic flow portion of the true-stress (σ_t)/true-plastic-strain (ϵ_p) curve can be represented by the familiar power law equation:

$$\sigma_t = K \epsilon_p^n \quad (1)$$

where

$$\begin{aligned} n &= \text{strain-hardening exponent} \\ K &= \text{strength coefficient} \end{aligned}$$

It should be noted that this representation is not a necessary requirement for determining the indentation-derived $\sigma_t - \epsilon_p$ data as will be shown later [Eqs. (2) and (3)], but it can be used to determine the strain-hardening exponent over the ϵ_p range of interest. Furthermore, a single power curve may not fit the entire $\sigma_t - \epsilon_p$ curve as noted in ASTM Standard E-646-78.

An appropriate program stored in the computer is used to solve the following equations and to thereby determine the flow curve from the ABI data.

$$\epsilon_p = 0.2 d_p/D \quad (2)$$

$$\sigma_t = 4P/\pi d_p^2 \delta \quad (3)$$

where

$$d_p = \{0.5 CD [h_p^2 + (d_p/2)^2] / [h_p^2 + (d_p/2)^2 - h_p D]\}^{1/3} \quad (4)$$

$$C = 5.47P(1/E_1 + 1/E_2) \quad (5)$$

$$\delta = \begin{cases} 1.12 & \phi \leq 1 \\ 1.12 + \tau \ln \phi & 1 < \phi \leq 27 \\ \delta_{\max} & \phi > 27 \end{cases} \quad (6)$$

$$\phi = \epsilon_p E_2 / 0.43 \sigma_t \quad (7)$$

$$\delta_{\max} = 2.87 \alpha_m \quad (8)$$

$$\tau = (\delta_{\max} - 1.12) / \ln(27) \quad (9)$$

In the above equation, σ_t is the true stress, ϵ_p is the true-plastic-strain, d_p is the plastic indentation diameter, D is the diameter of the ball indenter, P is the applied indentation load, h_p is the plastic indentation depth, E_1 is the elastic modulus of the test material, δ is a parameter whose value depends on the stage of development of the plastic zone beneath the indenter, α_m is a parameter proportional to the strain rate sensitivity of the test material or specimen (e.g., for low strain-rate-sensitive materials $\alpha_m = 1.0$), and "ln" is the natural logarithm.

The computer program is used to fit the ABI-derived $\sigma_t - \epsilon_p$ data [calculated using Eqs. (2) and (3)] by linear regression analysis to the relationship of Eq. (1), and determine the strain-hardening exponent (n) and the strength coefficient (K). The previous equations provide means for predicting the homogeneous portion of the stress/strain curve from indentation data.

A different approach must be used for measuring the yield strength of carbon steels (and other materials such as aluminum and titanium alloys) exhibiting inhomogeneous or Lüders strain. Similarly, methods of the prior art wherein the Lüders strain and yield strength are determined using either a profilometry or an optical interferometry technique, while suitable for laboratory applications, are not suitable for

infield applications because of their complexity.

In contrast, the information obtained using the FIM apparatus described above can be more easily and accurately used to obtain the yield strength of the test material using the following approach. For each ABI loading cycle the total penetration depth (h_t) is measured while the load is being applied, then converted to a total indentation diameter (d_t) using the following equation:

$$d_t = 2 (h_t D - h_t^2)^{0.5} \quad (10)$$

Data points from all loading cycles up to $d_t/D = 1.0$ are fit by linear regression analysis to the following relationship:

$$P/d_t^2 = A (d_t/D)^{m-2} \quad (11)$$

where P is the applied indentation load, m is Meyer's coefficient, and A is a test material (or specimen) parameter obtained from the regression analysis of test data of d_t/D versus P/d_t^2 . The test material parameter (A) is then used to calculate the yield strength (σ_y) of the material using the following empirical equation:

$$\sigma_y = \beta_m A \quad (12)$$

where β_m is a material-type constant (e.g., a single value of $\beta_m = 0.2285$ (Ref. 11) is applicable to all carbon steels whether cold rolled, hot rolled, or irradiated; other values of β_m for other types of material such as titanium alloys, aluminum alloys, etc., are stored in the computer). The value of β_m for each class or type of material is determined from regression analysis of tensile yield-strength values (measured from specimens with different heat treatments and flow properties and machined from different orientations) and their corresponding A values as measured from entire ABI curves (up to $d_t/D = 1.0$). In Eq. (12) above, the units of A and σ_y should be the same. The simplified and more accurate approach of the FIM invention to determine yield strength eliminates the determination of material pile-up except for residual stress evaluation and thereby significantly reduces testing time and thus cost.

For each loading cycle the total penetration depth (h_t) is measured while the load is applied and the plastic indentation depth (h_p) is measured after complete unloading. Since the unloading curve is fairly linear, and after comparing ABI test results using both complete and partial unloading cycles, ABI tests are now performed with partial unloading (e.g. see Fig. 6). The computer program used to control the test and analyze test data calculates the slope of each unloading cycle and then the intersection of this line with the zero load line (abscissa or X-axis) to determine the value of h_p . The material-type constant (β_m) of 0.2285 in Eq. (12) was determined by George et. al. (Ref. 11) from multiple Rockwell tests performed on steels with yield strength ranging from 193 to 655 MPa. This constant was found to produce good results using ABI test data.

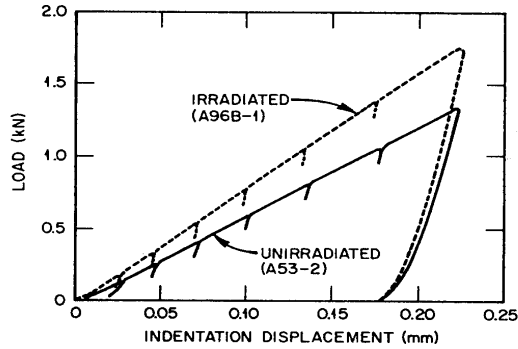


Fig. 6. Sample of ABI test results (load versus displacement using a 1.59-mm diameter ball indenter) on unirradiated and irradiated A212B pressure vessel steel specimens.

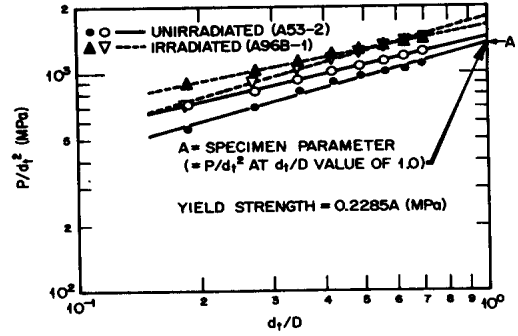


Fig. 7. Yield strength results calculated from the entire ABI load-displacement curve for two tests each conducted on unirradiated and irradiated A212B pressure vessel steel specimens.

Figure 7 shows the results of two ABI tests conducted on each of unirradiated and irradiated A212B steel specimens. The intersection of the log-log plot of P/d_1^2 (MPa) versus d_1/D with the vertical axis at $d_1/D = 1.0$ determines the material parameter "A" of Equation 12 in Table I. Multiplying this value of "A" by the constant of Equation 11 (0.2285) determines the value of the yield strength of the test material. Figure 7 also shows a graphical demonstration of the difference between the ABI-measured yield strength values of unirradiated and irradiated specimens. The irradiated specimen (A96B) was machined from a broken half of a CVN surveillance specimen irradiated in the HFIR reactor between 1965 and 1986. Another irradiated specimen, No. A31B, was irradiated in the HFIR between 1965 and 1983 in a different location where it accumulated a low fluence. The ABI tests conducted on this specimen did not show an increase in the yield

strength due to radiation-induced embrittlement, in agreement with the results of uniaxial tensile tests. A comparison between yield strength values measured using both uniaxial tensile tests and ABI tests is given in Table III. This table also shows that the difference between the average values of yield strength measured by ABI and tensile tests was less than 2%. The ABI-measured true-stress/true-plastic-strain curves of unirradiated and irradiated specimens are shown in Fig. 8. This figure shows that the irradiated (high fluence) specimen flow properties were higher than those of the unirradiated specimen over the entire curve. Furthermore, the ABI-measured flow properties showed an excellent agreement with those measured from a uniaxial tensile test as shown in Fig. 9. The strain-hardening exponent measured for these two irradiated specimens of Fig. 9 using ABI and tensile tests are 0.192 and 0.195, respectively.

Table I. Comparison of Yield Strength Results Measured by Uniaxial Tensile and ABI Tests on A212 Grade B Steel.

Fluence, >1 MeV ($n/cm^2 \times 10^{17}$)	Uniaxial Tensile		Automated Ball Indentation		B-A A (%)
	Specimen Number	Yield Strength (Mpa)	Specimen Number	Yield Strength (Mpa)	
			Average (A)	Average (B)	
0.0	A59-HA-15	336		333	
0.0	A59-HA-1	318	329	312	-1.8
0.00	A59-HA12	333			
0.12	A31-3	333		340	
0.12	A31-4	334	329	325	+1.2
0.12	A31-1	331			
0.12	A31-2	318			
1.53	A96-4	396		410	
1.53	A96-2	373	389	377	+1.3
1.53	A96-1	394			
1.53	A96-3	392			

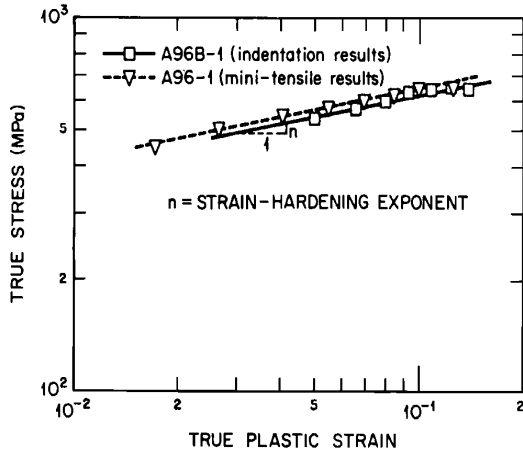


Fig. 8 Flow properties measured from ABI tests on unirradiated and irradiated A212B pressure vessel steel specimens (note that each curve is entirely obtained from multiple indentations at a single penetration location).

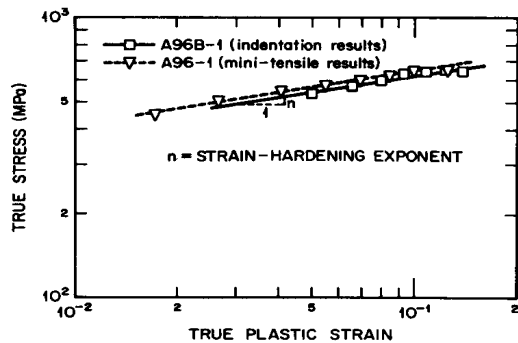


Fig. 9 Comparison between flow properties (true-stress/true-plastic-strain curve) measured from ABI and uniaxial tensile tests on irradiated A212B pressure vessel steel.

The results of the ABI tests were accurate, repeatable, reproducible, and showed excellent agreement with the results from standard tensile tests.

Although the average difference between the yield strength of the highly irradiated and the unirradiated A212B steel specimens was small (60 MPa) as measured by tensile tests, almost the same difference was measured by the ABI tests (71 MPa). This is very important since the change in yield strength can be used to predict the corresponding changes in the transition temperature shift of reactor pressure vessel steels (Reference 13). Full automation of the ball indentation test made it accurate, simple, fast (less than 10 minutes per test), and economic (cheaper than a destructive tensile test) for both field and laboratory applications. Other successful applications of the ABI include the characterization of welds (Ref. 14) and new alloys.

CONCLUSIONS

1. A field indentation microprobe (FIM) was conceived for evaluating the structural integrity of metallic components in-situ in a nondestructive manner.

2. The laboratory version of the FIM used in this work performed successful automated ball indentation (ABI) tests on both

unirradiated and irradiated A212B reactor pressure vessel steel specimens. Excellent agreement was obtained between flow properties measured by both uniaxial tensile and ABI tests.

3. The results also demonstrated that the laboratory ABI technique affords a simple, rapid, accurate, and nondestructive method of determining the flow properties of metallic alloys. Such a technique should be readily adaptable for field applications.

4. The FIM apparatus should be useful in mapping out localized changes in the mechanical and physical properties of deformed, aged, and embrittled structural components.

ACKNOWLEDGMENT

The authors gratefully acknowledge the excellent work of J. T. Hutton in the software development for this project.

This work was partially supported by the Office of Nuclear Regulatory Research, Division of Engineering, U. S. Nuclear Regulatory Commission under Interagency Agreement DOE 1886-8011-9B with the U.S. Department of Energy under contract DE-AC05-84OR21400 with Martin Marietta Energy Systems, Inc.

REFERENCES

1. Haggag, F. M., "Field Indentation Microprobe for Structural Integrity Evaluation," patent is pending, 1988.
2. Haggag, F. M. and Nanstad, R. K., "Estimating Fracture Toughness Using Tension or Ball Indentation Tests and a Modified Critical Strain Model," to be presented at the ASME Pressure Vessel and Piping Conference, Honolulu, July 23-27, 1989.
3. Cheverton, R. D., Merkle, J. G., and Nanstad, R. K., "Evaluation of HFIR Pressure-Vessel Integrity Considering Radiation Embrittlement," ORNL/TM-10444, April 1988.
4. Nanstad, R. K. et al., "Accelerated Neutron Embrittlement of Ferritic Steels at Low Fluence: Flux and Spectrum Effects," Journal of Nuclear Materials, 158 (1988) pp. 1-6.
5. Cheverton, R. D. et al., "Impact of Radiation Embrittlement on Integrity of Pressure Vessel Supports for Two PWR Plants," submitted for publication in the Proceedings of the 16th Water Reactor Safety Information Meeting, October 24-27, 1988, Gaithersburg, MD.
6. Haggag, F. M. and Lucas, G. E., "Determination of Luders Strains and Flow Properties in Steels from Hardness/Microhardness Tests," Metallurgical Transactions A, 14A, (1983), pp.1607-1613.
7. Haggag, F. M., "The Role of Luders Strain in Predicting Flow Properties in Steels from an Instrumented Hardness Test," M.S. Thesis, department of Chemical and Nuclear Engineering, University of California, Santa Barbara, CA. 1980.
8. Au, P., et al., "Flow Property Measurements from Instrumented Hardness Tests," Non-destructive Evaluation in the Nuclear Industry, Metals Park, OH., 1980, pp. 597-610.
9. Tabor, D., "The Hardness of Metals," Clarendon Press, Oxford, 1951.

10. Francis, H. A., "Phenomenological Analysis of Plastic Spherical Indentations," Transactions of the ASME, July 1976, p. 272-281.

11. George, R. A., Dinda, S., and Kasper, A. S., "Estimating Yield Strength from Hardness Data", Metal Progress, May 1976, pp. 30-35.

12. Haggag, F. M., et.al., "The Use of Automated Ball Indentation Testing to Measure Flow Properties and Estimate Fracture Toughness in Metallic Materials," to be presented at the ASTM Symposium on the Application of Automation Technology to Fatigue and Fracture Testing, Kansas City, Missouri, May 23-24, 1989.

13. Odette, R. G., et. al., "Relationship Between Irradiation Hardening and Embrittlement of Pressure Vessel Steels," Effects of Radiation on Materials: Twelfth International Symposium, ASTM STP 870, F. A. Garner and J. S. Perrin, Eds., American Society for Testing and Materials, Philadelphia, 1985, pp. 840-860.

14. Haggag, F. M., Nanstad, R. K., and Alexander, D. J., "The Use of Field Indentation Microprobe in Measuring Mechanical Properties of Welds," to be presented at the 2nd International Conference on "Trends in Welding Research," May 14-18, 1989, Gatlinburg, Tennessee.